

## Heparan Sulfate Proteoglycans Are Required for Cellular Binding of the Hepatitis E Virus ORF2 Capsid Protein and for Viral Infection<sup>∇†</sup>

Manjula Kalia,\* Vivek Chandra, Sheikh Abdul Rahman, Deepak Sehgal,# and Shahid Jameel

*International Centre for Genetic Engineering & Biotechnology, New Delhi, India*

Received 7 April 2009/Accepted 30 September 2009

**The hepatitis E virus (HEV), a nonenveloped RNA virus, is the causative agent of hepatitis E. The mode by which HEV attaches to and enters into target cells for productive infection remains unidentified. Open reading frame 2 (ORF2) of HEV encodes its major capsid protein, pORF2, which is likely to have the determinants for virus attachment and entry. Using an ~56-kDa recombinant pORF2 that can self-assemble as virus-like particles, we demonstrated that cell surface heparan sulfate proteoglycans (HSPGs), specifically syndecans, play a crucial role in the binding of pORF2 to Huh-7 liver cells. Removal of cell surface heparan sulfate by enzymatic (heparinase) or chemical (sodium chlorate) treatment of cells or competition with heparin, heparan sulfate, and their oversulfated derivatives caused a marked reduction in pORF2 binding to the cells. Syndecan-1 is the most abundant proteoglycan present on these cells and, hence, plays a key role in pORF2 binding. Specificity is likely to be dictated by well-defined sulfation patterns on syndecans. We show that pORF2 binds syndecans predominantly via 6-O sulfation, indicating that binding is not entirely due to random electrostatic interactions. Using an *in vitro* infection system, we also showed a marked reduction in HEV infection of heparinase-treated cells. Our results indicate that, analogous to some enveloped viruses, a nonenveloped virus like HEV may have also evolved to use HSPGs as cellular attachment receptors.**

Hepatitis E virus (HEV), the causative agent of hepatitis E, is responsible for sporadic infections as well as large outbreaks of waterborne acute hepatitis (9). It is a nonenveloped and single- and positive-stranded RNA virus of about 27 to 34 nm (30). The virus has been classified as the sole member of the genus *Hepevirus*, family *Hepeviridae* (15). The viral genome consists of short 5' and 3' untranslated regions and three open reading frames (ORFs), called ORF1, ORF2, and ORF3 (62). ORF1 encodes the nonstructural proteins that are involved in virus replication and viral protein processing (1, 56), ORF2 encodes the viral capsid protein, and ORF3, which overlaps the 5' end of ORF2 (62), encodes a small protein shown to regulate the cellular environment (8, 29, 44). The AUG start codon of ORF3 was predicted to overlap with the UGA stop codon of ORF1; however, recent studies have shown that the third in-frame AUG in the junction region is the authentic initiation site of ORF3 and is critical for virus infection (19, 26). Thus, ORF2 and ORF3 are proposed to be translated from a single bicistronic mRNA and overlap each other, but neither overlaps ORF1.

Until recently due to the lack of a suitable cell culture system or small animal models for the propagation of HEV, studies concerning the properties of individual gene products and their role(s) in replication were restricted to subgenomic or replicon

expression strategies. Viral genomic RNA is infectious for some cultured cells and nonhuman primates, and transfection with capped recombinant genomes can generate infectious virions (16, 47). It is now well established that HEV causes a zoonotic infection, and pigs and chickens are reservoirs for HEV (22, 42, 43). Hence, it is now possible to study HEV pathogenesis by using these animals as disease models. A recent study has examined the role of the hypervariable region of ORF1 in replication and pathogenesis of HEV in chicken and pigs by using species-specific infectious clones (50).

The ORF2 of HEV encodes its major capsid protein (pORF2) of 660 amino acids. This protein has been expressed using various *in vitro* systems and is also the basis for a recombinant subunit vaccine against hepatitis E. In animal cells, pORF2 is expressed in a 74-kDa form and an 88-kDa glycosylated form (gpORF2). Three N-linked glycosylation sites on pORF2 have been mapped to asparagine (Asn) residues at positions 137, 310, and 562 (70). A study using *in vitro* transcripts from an infectious cDNA clone mutated to eliminate potential glycosylation sites showed that none of the mutations affected genome replication or capsid protein synthesis in cell culture. However, these mutants were noninfectious, indicating that glycosylation of the capsid protein is biologically relevant (20).

In insect cells, the recombinant ORF2 protein of 72 kDa is proteolytically processed into 63-, 56-, and 53-kDa proteins containing a common N terminus starting at amino acid (aa) 112 but with different C termini. The 56-kDa truncated protein (aa 112 to 607) can self-assemble to form virus-like particles (VLPs) (34, 55), which, except for their smaller size, are morphologically similar to the native virus particle and possess dominant antigenic epitopes (34).

The antigenic composition of HEV proteins has been examined with synthetic peptides and recombinant proteins of dif-

\* Corresponding author. Mailing address: Virology Research Group, International Centre for Genetic Engineering and Biotechnology (ICGEB), Aruna Asaf Ali Marg, New Delhi 110 067, India. Phone: 91-11-26742357, ext. 251. Fax: 91-11-26742316. E-mail: manjula@icgeb.res.in.

# Present address: Biopharmaceuticals, R&D, Panacea Biotech Ltd., Mohan Cooperative Industrial Estate, New Delhi, India.

† Supplemental material for this article may be found at <http://jvi.asm.org/>.

<sup>∇</sup> Published ahead of print on 7 October 2009.

ferent sizes expressed in *Escherichia coli* (54). Expression of a truncated pORF2 (aa 394 to 660) results in the presentation of conformational epitopes. The shortest peptide reactive with neutralizing monoclonal antibodies (MAbs) was found to span aa 458 to 607 and is named the "neutralization peptide." This region appears to be critical, as removal of only a few amino acids from either end abrogates its recognition by neutralizing antibodies (71). Despite a number of studies on the antigenic domains of the ORF2 protein, the cellular receptor for HEV, its mode of infection, and viral determinants of attachment and infection remain unidentified.

Recently, two groups have reported the crystal structure of HEV-like particle (HEV-LP) (21, 69). Both studies show that the HEV-LP has three structural elements: an inner-shell domain that serves as an internal scaffold and forms a jelly roll-like  $\beta$ -sandwich, a middle domain that has a twisted antiparallel  $\beta$ -barrel structure, and the protruding domain that encompasses aa 456 to 606 and forms spikes. The protruding domain is dimeric and, being highly exposed, plays a major role in antigenicity determination and virus neutralization (21). Another group has reported the crystal structure of the HEV antigenic domain spanning aa 455 to 602 of the ORF2 protein (33). Dimerization of this domain is a prerequisite for virus-host interaction and binding of neutralizing antibodies. These structural studies are relevant to understanding the molecular mechanisms of HEV assembly and entry.

A number of viruses utilize cell surface heparan sulfate (HS) proteoglycans (PGs; HSPGs) as attachment factors. These include the herpes simplex virus (HSV) (58, 67), vaccinia virus (11), Sindbis virus (6), respiratory syncytial virus (32), noroviruses (63), adeno-associated virus (13), flaviviruses such as dengue virus (10), hepatitis C virus (3), and tick-borne encephalitis virus (39), and retroviruses such as human immunodeficiency virus type 1 (HIV-1) (45) and the human T-cell leukemia virus (48). The HSPGs also interact with numerous biological effector molecules, such as growth factors and their receptors, extracellular matrix proteins, and cell-cell adhesion molecules, and are known to provide docking sites for the binding of various enveloped viruses and other microorganisms to eukaryotic cells (5). The HSPGs are present almost ubiquitously on cell surfaces but are extensively heterogeneous with respect to their compositions and quantities among different species, cell types, tissues, and developmental stages. HS is found consistently on members of two major families of membrane-bound PGs: the transmembrane syndecans and glycosylphosphatidylinositol (GPI)-anchored glypicans. The PG core protein is often expressed on mammalian cells in a tissue-specific manner. The HS is a repeating, highly negatively charged, linear polymer of 30 to 400 variously sulfated uronic acid and glucosamine residues (17). During and after assembly, individual saccharide units are subjected to variable enzymatic modifications, which ultimately generate the HS fine structure. These variations include modifications in the length, degree of sulfation, and positions of the sulfate groups in the disaccharide repeats (35). In many cases, the binding of a particular ligand to HS depends on its specific modification pattern (37). It has been proposed that the tissue tropism of some viruses may be determined by the HS fine structure (51, 60).

In the present study, we demonstrated that the capsid ORF2 protein of HEV interacts with highly sulfated HSPGs on the

surface of Huh-7 liver cells. We have characterized the HSPG profile of these cells and observed that Syndecan-1 is the most abundantly expressed PG. We showed the specificity of binding to be dictated mainly by the 6-O sulfation of syndecans. Using a replicon-based *in vitro* infection system, we also showed that the HSPGs are required for HEV infection of liver cells.

## MATERIALS AND METHODS

**Reagents and cell lines.** Huh-7 and S10-3 (a subclone of human hepatoma cell line Huh-7; a kind gift from Suzanne Emerson, NIAID, NIH) cells were grown as a monolayer in Dulbecco's modified Eagle's medium (DMEM) supplemented with 10% fetal bovine serum. Heparin-agarose beads, heparin sodium salt, HS sodium salt (from bovine kidney), dextran sulfate, chondroitin sulfate A sodium salt (from bovine trachea), chondroitin ABC lyase, heparinase I, sodium chlorate, and SYBR green I were obtained from Sigma-Aldrich Chemicals (St. Louis, MO). A panel of differentially derived heparins, which included oversulfated (OS) heparin, OS heparan sulfate, 2-O-desulfated heparin, 6-O-desulfated heparin, and fully de-O-sulfated heparin, was obtained from Neoparin Inc. (Alameda, CA). The anti-HS antibody F58-10E4 and anti-del-HS antibody F69-3G10 were obtained from the Seikagaku Biobusiness Corporation, Japan (marketed by Cape Cod Inc., East Falmouth, MA). The anti-Syndecan-1 and anti-Syndecan-4 antibodies were obtained from Zymed Laboratories (Invitrogen Corporation, CA). The anti-Syndecan-2 and anti-Syndecan-3 antibodies were purchased from Santa Cruz Biotechnology, Inc., CA. The small interfering RNA (siRNA) reagents against Syndecan-1 and Syndecan-4 were obtained from Dharmacon Inc. (Thermo Scientific). The anti-ORF2 antibody has been described earlier (27). Alexa 488/594-coupled anti-rabbit and anti-mouse antibodies and ProLong Gold antifade reagent with DAPI (4',6-diamidino-2-phenylindole) were obtained from Invitrogen Corporation, NY. Alexa 647-conjugated anti-CD59 and phosphatidylinositol phospholipase C (PIPLC) were a kind gift from Satyajit Mayor (NCBS, Bangalore, India). The T7 Riboprobe *in vitro* transcription system and the Ribo m<sup>7</sup>G cap analog were obtained from Promega Pte. Ltd. (Singapore).

**Generation of ORF2 proteins.** The 56-kDa ORF2 protein was purified following expression through a baculovirus system by using the insect cell line Tn5 (Invitrogen, Carlsbad, CA) as described earlier (57). For the generation of the aa 458 to 607 ORF2 polypeptide, the region was PCR amplified and cloned into the prokaryotic expression vector pRSET. After transformation into *E. coli* BL21(DE3) and induction with IPTG (isopropyl- $\beta$ -D-thiogalactopyranoside), the protein was purified by Ni-nitrilotriacetic acid affinity chromatography on His-Bind resin (Qiagen, Germany) according to the manufacturer's protocol.

**Sedimentation analysis of pORF2 by sucrose density gradients.** The purified pORF2 was tested for its ability to be pelleted in a 20% sucrose cushion. The ORF2 protein (40  $\mu$ l of 1 mg/ml) was loaded on top of a 4.3-ml 20% sucrose cushion and subjected to ultracentrifugation at 35,000 rpm (164,000  $\times$  g) for 16 h at 4°C in a Beckman SW60 Ti rotor. The pellet was suspended in phosphate-buffered saline (PBS) and was analyzed by sodium dodecyl sulfate-polyacrylamide gel electrophoresis (SDS-PAGE) and Western blot analysis for ORF2. To determine the buoyant density of the purified pORF2, an isopycnic centrifugation in a sucrose density gradient (20%-60%) was performed. Briefly, a sucrose gradient was prepared in Beckman ultracentrifuge SW60 Ti tubes by layering 2.2 ml of 20% sucrose on top of 2 ml 60% sucrose. The ORF2 protein (1 mg/ml) was layered on top in a volume of 40  $\mu$ l. Centrifugation was carried out as described above, and six fractions of 0.7 ml each were collected from the top. The 20%-60% interface was collected in fraction 4. The fractions were run on SDS-PAGE and Western blotted with anti-pORF2 antibodies.

**pORF2-heparin interaction studies.** HEV pORF2 (40  $\mu$ g) or bovine serum albumin (BSA) (40  $\mu$ g) was allowed to bind to 100  $\mu$ l of heparin-agarose beads for 2 h at 4°C. The beads were washed thrice with PBS, and the bound protein was eluted by direct addition of 2 $\times$  Laemmli SDS-PAGE buffer. The eluted fractions were analyzed by SDS-PAGE, Coomassie staining, and Western blotting for ORF2. In a parallel experiment, after binding to heparin-agarose beads, the protein was eluted with a stepwise 0.1-to-0.6 M NaCl gradient and analyzed by SDS-PAGE and Western blotting for pORF2.

**Analysis of ORF2 protein binding to cells by flow cytometry.** Cells were detached from culture dishes with PBS containing 5 mM EDTA for 10 min at 37°C, pelleted at 400  $\times$  g for 5 min and resuspended in cold PBS supplemented with 1% BSA (wash buffer). The cells were incubated with pORF2 (20  $\mu$ g/ml) for 30 min on ice and washed twice with wash buffer followed by fixation with 2% paraformaldehyde. Fixed and washed cells were stained with anti-pORF2 antibody (1/1,000 dilution) and Alexa 488 anti-rabbit secondary antibody (1/500 dilution). For enzyme pretreatment, Huh-7 cells were removed from culture

plates as described above and incubated with heparinase I (5 U/ml), for 1 h at 37°C. The pORF2 binding and staining were then done as described above. For a control, cells were also stained with the primary and secondary antibodies without prior pORF2 binding. Acquisition was done on a FACSCalibur flow cytometer (Becton Dickinson), and data were analyzed using the Flow-Jo software (Tree Star, Inc.).

**Detection and quantitation of pORF2 binding by immunofluorescence.** For imaging studies, cells were grown on coverslips, and purified recombinant pORF2 was added at different concentrations ranging from 20 to 100 µg/ml. Binding was carried out on ice for 30 min, following which cells were washed extensively with chilled PBS and fixed with 2% formaldehyde. Staining was done using anti-pORF2 polyclonal antibody (1/1,000 dilution) and Alexa 488/594-coupled anti-rabbit secondary antibody (1/500 dilution). Coverslips were mounted in ProLong antifade containing DAPI. Imaging was done with 20×/40×/60× objectives on a Nikon A1-R confocal microscope. For the effects of heparinase I or chondroitin ABC lyase, cells were treated with the enzyme at 37°C for 1 h, following which pORF2 binding studies were performed. For studies with various glycosaminoglycans (GAGs), pORF2 was preincubated with defined GAGs at various concentrations for 20 min at room temperature. The protein-GAG complexes were then added to cells, and cellular binding was assessed. For quantitative measurement studies, images were acquired at 40× on the Nikon A1-R microscope. In each experiment, fluorescence was calculated from 10 to 12 fields (100 to 120 cells) from duplicate slides for each inhibitor concentration. Total fluorescence of cells was determined by marking out a cell outline from the digital interference contrast image, and the fluorescence intensity value per cell was obtained using Metamorph software (Universal Imaging Corporation). Integrated values of cell fluorescence were corrected for background autofluorescence. The weighted mean value and the uncertainty in the mean were determined on a per-field basis, considering each field (consisting of 5 to 20 cells) to be an independent event. For a control, background binding of BSA (instead of pORF2) to cells was determined. Intensity measurements of pORF2 binding in the presence of inhibitors were normalized, considering pORF2 binding in the absence of inhibitors as 100%.

**Inhibition of cellular GAG sulfation by sodium chlorate.** To reduce the extent of sulfation on HSPGs, Huh-7 cells were cultured for 48 to 96 h in DMEM (Invitrogen) containing 10% fetal bovine serum (FBS) in the presence of sodium chlorate at concentrations ranging from 25 mM to 75 mM. Sodium chlorate is a potent inhibitor of all cellular sulfation reactions but has no effect on protein synthesis or other posttranslational modifications.

**In vitro HEV replicon transfection of cells.** Plasmid pSK-E2 was linearized at a unique BglII site located immediately downstream of the HEV poly(A) tract, and capped transcripts were synthesized as previously described (8, 16). Transcription mixtures were cooled on ice and mixed with a liposome mixture consisting of 25 µl of DMRIE-C (1,2-dimyristyloxypropyl-3-dimethyl-hydroxy ethyl ammonium bromide and cholesterol; Invitrogen, Carlsbad, CA) in 1 ml of Opti-MEM. This was added to a T25 flask containing washed S10-3 cells at 40% confluence. The flasks were incubated at 34.5°C for 6 h, an additional 1 ml of Opti-MEM was added, and incubation was continued overnight. Cells were then trypsinized, split into two T25 flasks, and incubated in DMEM containing 10% FBS. On day 8 posttransfection, cells were again trypsinized and centrifuged. The supernatant was aspirated, and the cell pellet was stored at -80°C. Frozen pellets were extracted at room temperature by adding 0.9 ml of water per T25 pellet and vortexing vigorously until the pellet dispersed and the solution became cloudy. The sample was vortexed once or twice more in the next 10 min, 0.1 ml of 10-times-concentrated PBS was added, and debris was removed by centrifugation at 15,700 × g for 2 min. The supernatant was removed, placed on ice, and taken as a source of virions.

**In vitro infectivity assay and real-time RT-PCR.** The S10-3 cells at 60% confluence in 12-well plates were incubated with different amounts of heparinase I as indicated or with PBS as a control at 37°C in a 5% CO<sub>2</sub> atmosphere. After a 1-h incubation, cells were washed twice with PBS, 0.2 ml of virion mix was added, and the mixture was incubated at 37°C in a 5% CO<sub>2</sub> atmosphere for 2 h, after which the liquid was replaced with 1 ml of growth medium containing antibiotics. Two days postinfection, the cells were trypsinized, split into 2 wells of the 12-well plate, and incubated in DMEM containing 10% FBS. Five days postinfection, the cells were washed twice with PBS, and total RNA was isolated using the Trizol reagent (Invitrogen, Carlsbad, CA). Two micrograms of RNA in a 25-µl reaction mixture was used for cDNA synthesis with reverse transcriptase (RT; Promega, Madison, WI) according to the supplier's protocol by using primer EU4 (5'-GCCTGCGCGCCGGTGCACAACA-3') for ORF2 and oligo(dT) for the histone H4 control. Of this, 2 µl of the cDNA mixture was used as a template for PCR amplification of the target gene, ORF2. The PCRs were performed in a 50-µl volume containing 1× reaction buffer, 200 µM (each)

deoxynucleoside triphosphates, 10 pmol of each primer, and 1.25 U of *Taq* DNA polymerase (Real Biotech Corporation, Taipei, Taiwan) for 25 cycles of 94°C for 30 s, 55°C for 30 s, 72°C for 30 s, and a final extension at 72°C for 5 min. The primers used for PCR were EU2 (5'-TGGAGAATGCTCAGCAGATAA-3') and EU3 (5'-TAAGTGGACTGGTCGTACTIONCGGC-3'). From this, 2 µl of the amplified product was used as a template and reamplified for another 20 cycles. As a control for RNA loading, histone H4 RT-PCR amplification was performed as described earlier (44). For real-time PCR amplification, SYBR green I was used to monitor the amplification. The real-time PCRs were performed using the 2 µl of the amplified product in a 25-µl volume containing 0.5× SYBR green, 1× reaction buffer, 200 µM (each) deoxynucleoside triphosphates, 5 pmol of each primer, 5% dimethyl sulfoxide, and 1 U of *Taq* DNA polymerase (Real Biotech Corporation, Taipei, Taiwan) for 40 cycles of 95°C for 30 s, 55°C for 30 s, 72°C for 30 s, and a final extension at 72°C for 5 min. The real-time fluorescence signal generated was analyzed using the iCycler software. The threshold fluorescence level was automatically set by the software, and the threshold cycle (*C<sub>T</sub>*) was determined for each sample. For all assays, a melting curve from 60°C to 100°C was recorded. A negative control without DNA template and positive control with pSK-E2 plasmid were run with every assay to assess the overall specificity.

## RESULTS

**Characterization of the ORF2 56-kDa VLP generated in baculovirus.** The 56-kDa HEV ORF2 protein was checked for its capacity to form VLPs. The ORF2 protein could be pelleted through a 20% sucrose cushion (see Fig. S1A, lane 8, in the supplemental material), indicating the formation of a VLP. The protein was also subjected to sucrose equilibrium gradient centrifugation localized to fractions at or near the 20%-60% sucrose interface (see Fig. S1A, lanes 1 to 6, in the supplemental material), confirming the assembly of VLPs. The densities of the fractions demonstrating immunoreactivity for pORF2 were measured to be 1.12 to 1.22 g/cm<sup>3</sup>. These studies established that the 56-kDa pORF2 used later in these studies assembled as VLPs.

**The HEV ORF2 protein binds to HSPGs on Huh-7 cells.** The 56-kDa HEV ORF2 VLPs were found to attach as punctate structures all over and just outside the cellular membrane of Huh-7 cells (Fig. 1A). The punctate staining pattern for pORF2 suggested binding to some ubiquitous molecules on cells, such as HSPGs, which could also be shed into the medium. To check if pORF2 bound to Huh-7 cells through HSPGs, cells were treated with heparinase I, an enzyme which degrades heparin and highly sulfated domains in heparin sulfate (36). This reduced the binding of pORF2 to nearly control levels in cells (Fig. 1B and C). This result is consistent with HSPGs being attachment receptors for pORF2 on Huh-7 cells. This was also evident from a flow cytometric analysis of pORF2 binding to control and heparinase-treated Huh-7 cells (Fig. 1D). We also tested an aa 458 to 607 ORF2 polypeptide expressed in bacteria for its binding to Huh-7 cells. This ORF2 polypeptide was reported to be recognized by anti-HEV neutralizing antibodies, and the critical receptor binding domain of HEV was proposed to lie within this region (71). We observed no binding of this polypeptide to Huh-7 cells (data not shown), suggesting that binding of pORF2 to HSPGs is either mediated by determinants that are outside the aa 458 to 607 region or by positively charged residues that are brought together in the VLP structure to create an HSPG binding motif.

Since the pORF2 VLP showed HSPG binding on cells, the heparin-binding activity of pORF2 was directly examined by incubating the protein with heparin-agarose beads (see Fig. S1B and C in the supplemental material). pORF2 showed

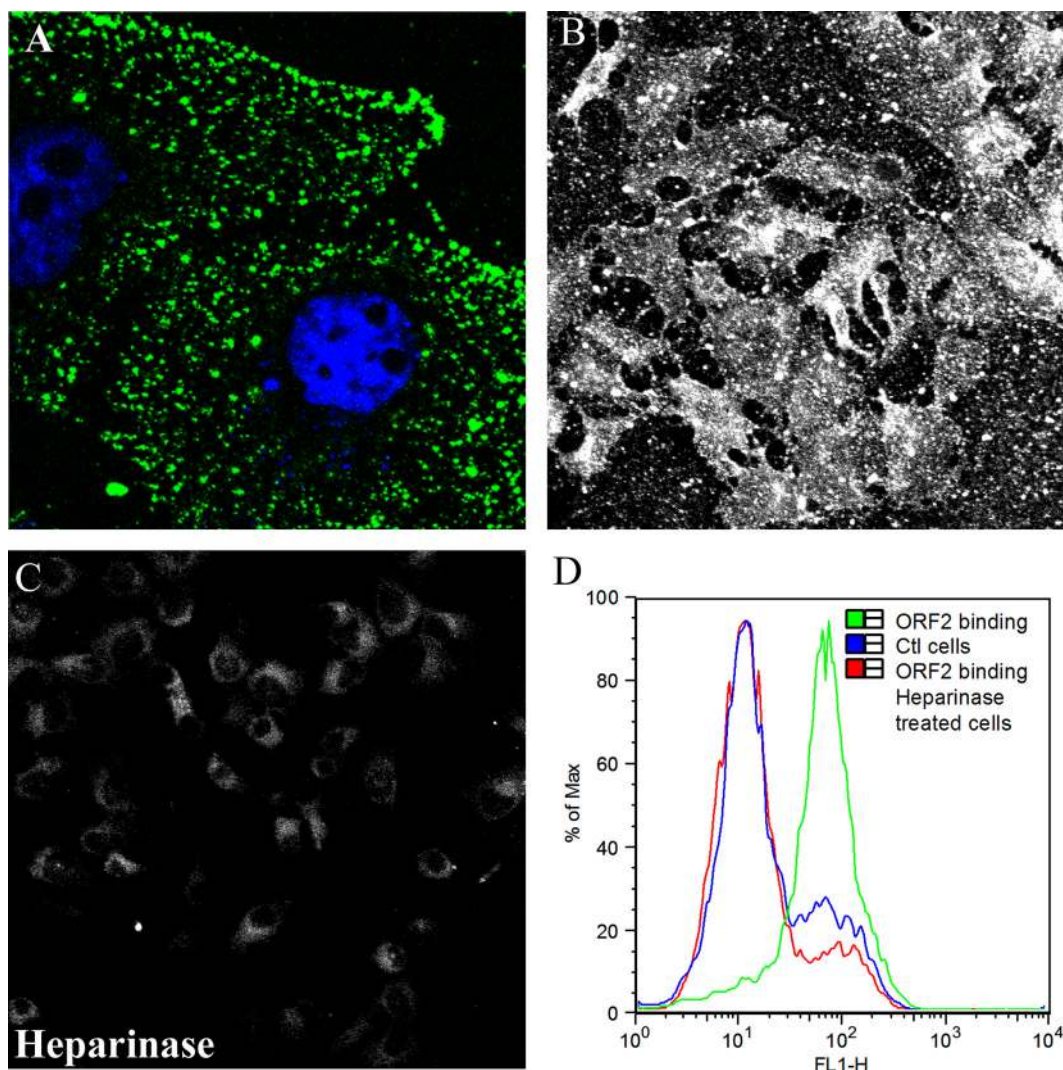


FIG. 1. The HEV ORF2 protein binds to HSPGs on Huh-7 hepatoma cells. (A) Recombinant ORF2 protein VLPs (20  $\mu\text{g}/\text{ml}$ ) were added to Huh-7 cells grown on coverslips for 30 min on ice. After being washed, cells were fixed and stained with anti-pORF2 and Alexa 488-conjugated anti-rabbit immunoglobulin G antibodies. Cells were also stained with DAPI and imaged at 60 $\times$ . Cell nuclei can be seen in blue (DAPI), and pORF2 can be seen in green. Huh-7 cells were either left untreated (B) or treated with 5 U/ml heparinase I (C) for 1 h at 37 $^{\circ}\text{C}$ . After the cells were washed, pORF2 (20  $\mu\text{g}/\text{ml}$ ) was added to cells for 30 min on ice. After being washed, cells were fixed and stained as described above and imaged at 20 $\times$ . (D) The binding of pORF2 to Huh-7 cells with or without heparinase treatment was also tested by flow cytometry as described in Materials and Methods. The histogram shown is representative of two independent experiments. Ctl, control; Max, maximum; FL1-H, ORF2 A488.

strong binding to heparin-agarose, whereas control protein BSA did not bind (see Fig. S1B in the supplemental material). The bound protein could be eluted from the heparin-agarose beads by using a stepwise salt gradient (see Fig. S1C in the supplemental material). Binding of pORF2 to heparin-agarose beads and its elution by 0.3 M and higher salt concentrations is clear evidence of a high-affinity interaction.

**The HSPG profiles of Huh-7 and S10-3 cells.** We determined the HSPG profiles of Huh-7 and S10-3 cells by using two MAbs, F58-10E4 and F69-3G10. The F58-10E4 MAb specifically recognizes intact HSPGs on the cell surface. On treatment with heparinase III, which removes HS chains from the core PG, the epitope recognized by F58-10E4 is eliminated, whereas the epitope recognized by the F69-3G10 antibody is

unmasked. When the Huh-7 cells were stained, a strong F58-10E4 signal was seen, and this was lost upon treatment with heparinase III (Fig. 2A). On the contrary, F69-3G10 staining, which was weak in untreated cells, increased significantly after digestion with heparinase III (Fig. 2B). The existence of HSPGs on these cells was further confirmed by Western blotting. Cells were treated with heparinase III to remove the HS chains, and the PGs were allowed to migrate in SDS-polyacrylamide gels according to the molecular mass of their protein cores. The HSPG cores were identified by Western blotting using F69-3G10, which specifically recognizes the HS "stub" left on PGs after heparinase digestion (12). The HS stub-bearing core proteins were visible as two prominent bands at 85 and 48 kDa, and other bands were seen at 60, 38, and 30

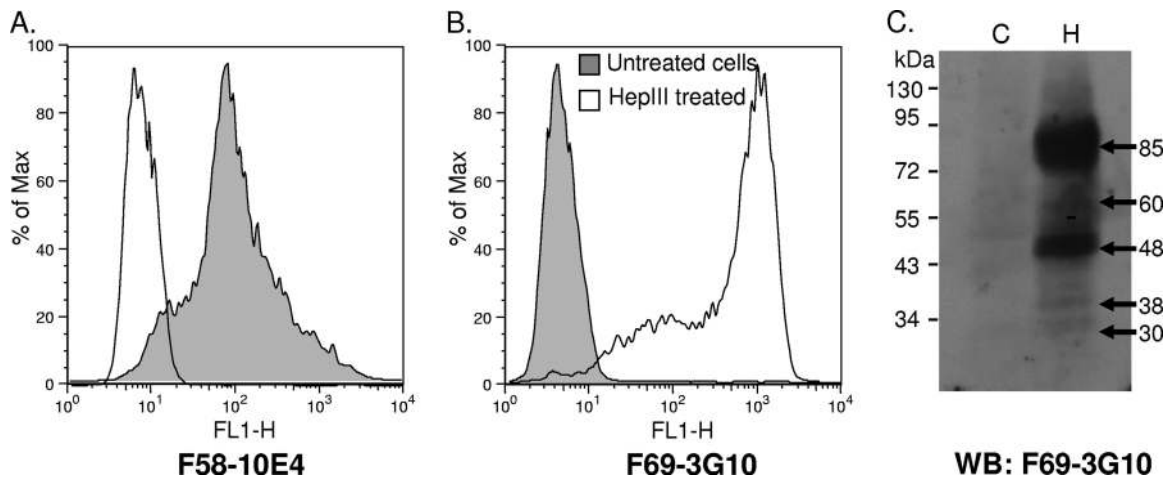


FIG. 2. HSPG profiles on Huh-7 and S10-3 cells. (A and B) Huh-7 cells were detached, left untreated or treated with the enzyme heparinase III (HepIII; 2.5 U/ml) for 1 h at 37°C, and stained with HSPG-specific MAb F58-10E4 or MAb F69-3G10, washed, and labeled with Alexa 488-conjugated anti-mouse secondary antibody. Cells were analyzed by flow cytometry as described in Materials and Methods. Max, maximum; FL1, anti-mouse Alexa 488. (C) Untreated or heparinase III-treated Huh-7 cells were lysed, cell lysates were separated with SDS-PAGE, and Western blotting (WB) was done with MAb F69-3G10, which recognizes the PG stub after heparinase treatment. Lane C, control cell lysate; lane H, heparinase III-treated lysate. The masses (in kDa) of the major bands seen in lane H are marked with an arrow.

kDa, indicating that multiple members of HSPG families are present on Huh-7 cells (Fig. 2C). The S10-3 cells also showed a similar expression pattern in flow cytometry and Western blotting analyses with these antibodies (data not shown).

**The HEV ORF2 protein binds syndecans.** The HSPGs are present on the cell surface as either transmembrane syndecans or GPI-anchored glypicans. Studies on syndecan expression in a number of tissues and cell lines have shown that virtually all cells express at least one form of syndecan, most cells express multiple forms, and there is a distinct pattern of syndecan expression that characterizes individual cell types and tissues (28). To test whether pORF2 binding is mediated by syndecans or glypicans, we treated cells with PIPLC, an enzyme that cleaves the GPI anchor. For a control for the activity of PIPLC, we tested binding of an Alexa 647-conjugated antibody against CD59, a GPI-anchored protein present on the surface of most cells. There was no difference between the binding of pORF2 in untreated cells and that in PIPLC-treated cells (Fig. 3A and E), whereas the binding of anti-CD59 was lost in PIPLC-treated cells, indicating cleavage of all membrane GPI-anchored proteins, including glypicans (Fig. 3B and F). This indicates that pORF2 binds to HS chains on the transmembrane-anchored syndecans and not on the GPI-anchored glypicans or that Huh-7 cells express very low levels of glypicans, which do not contribute significantly to pORF2 binding.

**Expression levels of syndecans on Huh-7 cells and their role in pORF2 binding.** We next analyzed syndecan expression on Huh-7 cells. According to published literature, the molecular weights of the HSPG cores correspond to molecular masses reported for Syndecan-1 (85 kDa), Syndecan-2 (48 kDa), Syndecan-3 (60 kDa), and Syndecan-4 (30 to 38 kDa). Accordingly, we tested antibodies against syndecans on Huh-7 cell lysates from both untreated and heparinase III-treated cells. Even though the F69-3G10 antibody detected all four putative syndecans (Fig. 2C), we were able to confirm the expression of only Syndecan-1 and Syndecan-4 by Western blotting (Fig. 4A

and B) on Huh-7 cells. These antibodies were also tested with flow cytometry (Fig. 4C) and immunofluorescence (see Fig. S2A and B in the supplemental material). In Western blots, the band corresponding to Syndecan-1 intensified greatly on heparinase III treatment, indicating that the epitope is more available for antibody binding after HS chain removal (Fig. 4A, compare lanes C and H). Despite generating an intense signal with antibody F69-3G10, the putative Syndecan-2 (migrating at 48 kDa) (Fig. 2C) did not react with the anti-Syndecan-2 antibody (data not shown). We were also not successful in immunoprecipitating Syndecan-2 from Huh-7 cells by using this antibody (data not shown). Our studies showed that Huh-7 cells express high levels of Syndecan-1 and lower levels of Syndecan-4. We further checked for the contributions of these syndecans in pORF2 binding by lowering their levels by RNA interference (see Fig. S2C and D in the supplemental material). Depletion of Syndecan-1 results in a nearly 70% reduction in pORF2 binding, whereas depletion of Syndecan-4 had only a negligible effect (Fig. 4D). These studies suggest that Syndecan-1, the most abundant PG on Huh-7 cells, contributes maximally to pORF2 binding. It is now well understood that syndecan type-specific differences do not contribute to HS fine structure. Structurally distinct forms of syndecans can be produced as a result of variations in the number, type, length, or fine structure of the attached GAG (7).

**Effect of various GAGs on pORF2 binding.** We then assessed the role of heparin and a series of soluble GAGs as possible competitive antagonists of pORF2 binding to Huh-7 cells. Although heparin is not a constituent of cell membranes, this molecule is a structural homolog of highly sulfated HS (46). Upon preincubation of pORF2 with heparin and OS heparin, there was a dose-dependent inhibition of pORF2 binding to Huh-7 cells (Fig. 5A). We also analyzed the potential role of HS as an inhibitor of pORF2 binding. While OS-HS strongly inhibited pORF2 binding to Huh-7 cells by up to 80%, the kidney-derived normally sulfated HS inhibited pORF2

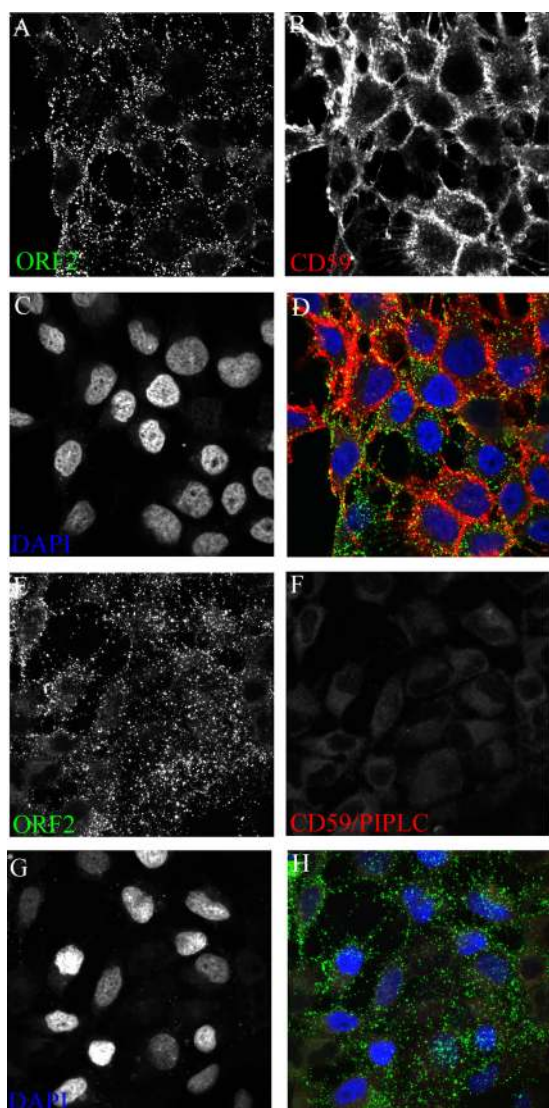


FIG. 3. Binding of pORF2 is mediated by transmembrane syndecans and not GPI-anchored glypicans. The ORF2 protein (20  $\mu\text{g}/\text{ml}$ ) was added to untreated (A to D) or PIPLC-treated (E to H) Huh-7 cells. Cells were costained with anti-pORF2 as described in the legend to Fig. 1 and with Alexa 647-conjugated anti-CD59 (marker of GPI-anchored proteins). After the nuclei were stained with DAPI, the images were acquired at 20 $\times$ . The merged pictures (D and H) show pORF2 (green), CD59 (red), and nuclei (blue).

binding only up to a maximum of 50%, even at the highest concentrations (Fig. 5B). These results suggest that the extent of PG sulfation was functionally important for pORF2 binding to Huh-7 cells. Kidney-derived HS represents a prototype for normally sulfated HSs, whereas liver-derived HS represents the highly sulfated form. The observation that kidney-derived HS is not as efficient an antagonist of pORF2 binding as OS-HS suggests that the degree of sulfation is important in mediating pORF2 binding on HSPGs.

The majority of GAG chains added to syndecan core proteins are HS chains, but some of these proteins bear chondroitin sulfate as well. The extracellular domains of syndecans bear HS chains that are distal and chondroitin sulfate chains

that are proximal to the plasma membrane. To test whether pORF2 binding was mediated by chondroitin sulfate, Huh-7 cells were treated with chondroitin ABC lyase, which specifically cleaves glycosidic linkages in chondroitin sulfates A, B, and C (68). Cells treated with chondroitin lyase showed about 35% inhibition of pORF2 binding, indicating a small contribution by chondroitin sulfate to the binding of pORF2 on cells as well (Fig. 5C). Coincubation of pORF2 with chondroitin sulfate A also did not have a significant effect on its binding to Huh-7 cells (Fig. 5C). However, dextran sulfate, a heavily sulfated and negatively charged glucose polysaccharide, markedly inhibited pORF2 binding to Huh-7 cells (Fig. 5C). Similar inhibition patterns were observed with all the reagents for the binding of pORF2 to S10-3 cells (subclones of Huh-7 cells) (data not shown). Soluble polyanions like dextran sulfate that are highly sulfated also tend to be good inhibitors of viruses that bind HSPGs, probably as a result of their interference with the electrostatic interactions that facilitate virus attachment and entry.

**Relevance of sulfation.** To further confirm that target cell sulfation is required for binding the HEV capsid protein, Huh-7 cells were cultured in low-sulfate medium together with sodium chlorate, a specific inhibitor of sulfation. The binding of pORF2 to Huh-7 cells was inhibited in a dose-dependent manner by culturing the cells in sodium chlorate (Fig. 6), again emphasizing the role of cell surface sulfation in pORF2 binding to Huh-7 cells.

**The ORF2 protein binds predominantly to 6-O-sulfate groups of HSPGs.** Studies reported here suggest that highly sulfated heparin sulfate motifs on syndecans serve as binding sites on liver cells for pORF2. We further analyzed the role of differentially desulfated heparins to test whether pORF2 binding to Huh-7 cells was specific or merely an electrostatic interaction. Distinct O sulfations on heparin have been shown to differentially contribute to the contact between a ligand and its receptor (14, 60). To understand finer details of the pORF2–Huh-7 interaction, we therefore tested various desulfated heparins in a competition assay. These included fully de-O-sulfated heparin in which all O-sulfate esters of heparan were removed without changing the backbone structure and most of the negative charges contributed by O sulfates were eliminated, 2-O-desulfated heparin from which only 2-O-sulfate esters were removed, and 6-O-desulfated heparin from which only 6-O-sulfate esters were removed. Fully O-desulfated heparin showed only 30 to 40% reduced binding, indicating that O sulfation contributes significantly to pORF2 binding to Huh-7 cells (Fig. 7B and E). This reduction could be due to the contribution of N sulfation or chondroitin sulfates. The 2-O-desulfated heparin effectively competed out pORF2 binding to Huh-7 cells (Fig. 7C and E), indicating that modifications other than 2-O sulfation are critical for binding. The 6-O-desulfated heparin showed only a partial inhibition of pORF2 binding (Fig. 7D and E), suggesting a key role for 6-O sulfation in the binding of pORF2 to Huh-7 cells. Recent binding studies with selected proteins have shown that a particular kind of sulfate group (e.g., 6-O sulfates) may contribute more to an interaction (2).

**HSPGs are required for HEV infection.** The binding of pORF2 to cells raises the question of whether HSPGs are sufficient to initiate the multistep process leading to infection

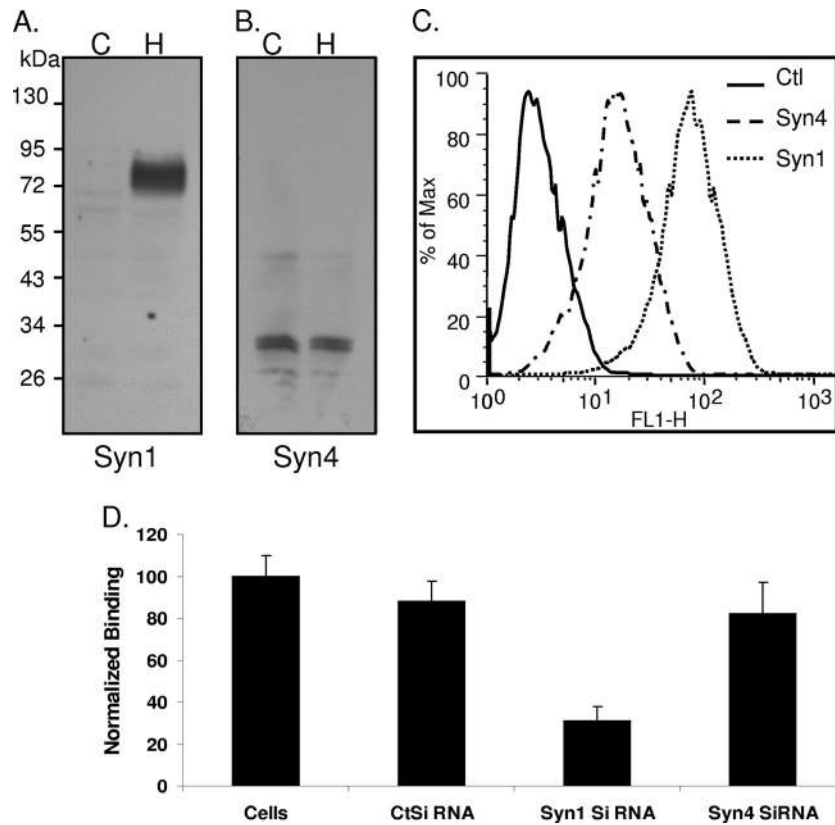


FIG. 4. Expression of Syndecan-1 (Syn1) and -4 (Syn4) on Huh-7 cells and the effect of their depletion on pORF2 binding. (A and B) Huh-7 cells left untreated (lanes C) or treated with heparinase III (lanes H) were lysed and Western blotted with anti-Syndecan-1 and anti-Syndecan-4 antibodies. The Syndecan-1-specific band is significantly enhanced under the heparinase III treatment condition, whereas Syndecan-4 was equally detectable in untreated and heparinase III-treated cells. (C) Flow cytometry profile of Huh-7 cells stained with Syndecan-1 and Syndecan-4. Huh-7 cells show much higher levels of Syndecan-1 than Syndecan-4. Max, maximum; Ctl, control; FL1, anti-rabbit Alexa 488. (D) Effects of Syndecan-1 and Syndecan-4 depletions by RNA interference on pORF2 binding on Huh-7 cells. Huh-7 cells were transfected with siRNA reagents specific for Syndecan-1 and Syndecan-4 and a nonspecific control siRNA (CtSi RNA). Maximal silencing of the genes was seen at 72 h posttransfection. Binding and analysis of pORF2 were performed as described in Materials and Methods.

and viral replication. To confirm the biological relevance of results obtained with the ORF2 protein, we carried out an *in vitro* infection experiment and asked whether HSPG removal would inhibit infection of hepatoma cells by HEV. For this, we utilized an infectious HEV replicon to produce the virus in S10-3 cells as described earlier (8, 16). The cell lysates prepared from replicon-transfected cells were used as a source of infectious HEV particles and tested for their ability to infect cells that were depleted of HSPGs by pretreatment with heparinase I. Successful infection was measured by RT-PCR for HEV RNA in the infected cells. The results are shown in Fig. 8A. Lysates prepared from mock-transfected cells showed no infection of target cells (Fig. 8A, second lane from the left), while the lysates prepared from replicon-transfected cells when applied to target cells showed infection, measured as RT-PCR amplification of HEV RNA (Fig. 8A, third lane). Importantly, infection of heparinase I-treated cells treated with the lysate of replicon-transfected cells (the same as in Fig. 8A, second lane) showed a significant reduction in HEV RNA amplification (fourth lane). To assess the effects of different concentrations of heparinase I treatment on HEV infectivity, we treated the cells with different amounts of heparinase I, and then infection was measured by real-time RT-PCR for HEV RNA in the

infected cells by using SYBR green I (Fig. 8B). The reduction of HEV infectivity started with 1 U of heparinase I treatment and reached saturation levels at 5 U of heparinase I treatment. When we compared the  $C_T$  values with a standard curve prepared using different amounts of the pSK-E2 plasmid (data not shown), an approximately 80% reduction in HEV infectivity was observed for 5 U heparinase I-treated cells compared to the amount for control cells (Fig. 8B). This strongly indicates that HSPGs are required for the infection of target cells with HEV.

## DISCUSSION

Attachment to cells often represents a crucial and limiting step in virus entry. Infection of cells by most viruses is a two-step or multistep process, with the initial contact through a high-density but low-affinity receptor like an HSPG, followed by transfer to a high-affinity receptor for internalization. Interaction with HSPGs leads to virus enrichment on the cell surface, allowing subsequent two-dimensional scanning for specific entry (18, 25, 41).

This study demonstrates that VLPs prepared from the ORF2 capsid protein of HEV associate with syndecans, a specific class of cell surface HSPGs. According to the general

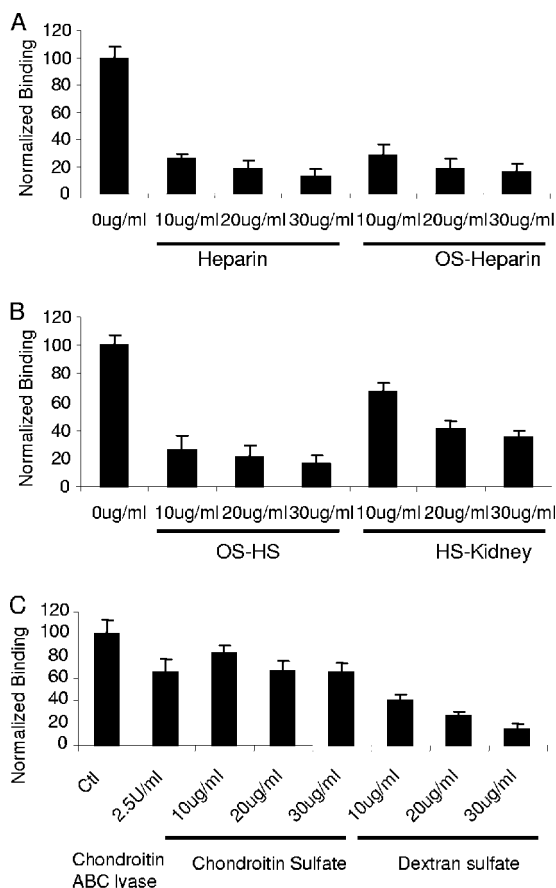


FIG. 5. Effects of GAGs and chondroitinase on pORF2 binding. The binding of pORF2 to Huh-7 cells was tested in the absence or presence of the indicated concentrations of heparin or OS heparin (A) and OS-HS or kidney-derived HS (HS-Kidney) (B). (C) Cells were treated with chondroitinase (2.5 U/ml) at 37°C for 1 h, or incubated with chondroitin sulfate or dextran sulfate at the indicated concentrations and ORF2 binding was done. After being washed, the cells were fixed and stained for pORF2 as described above. The images were acquired at 20×, and intensity measurements were made as described in Materials and Methods. Ctl, control.

concept of molecular recognition of HS/heparin by proteins, pORF2 binding to HS is likely to rely on an interaction between clusters of basic amino acids of pORF2 and negatively charged sulfate/carboxylate groups of HS/heparin. The HSPGs

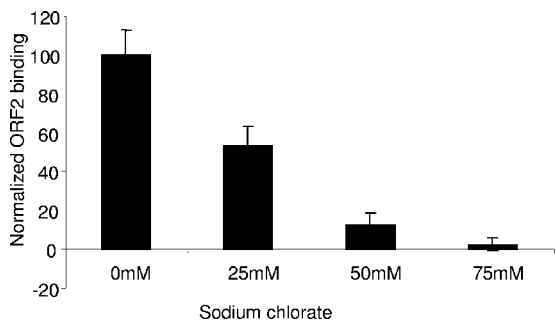


FIG. 6. The sulfation inhibitor sodium chlorate reduces pORF2 binding to Huh-7 cells. Huh-7 cells were grown for 48 h in the absence or presence of the indicated concentrations of sodium chlorate. The binding of pORF2 to these cells was assessed as described above.

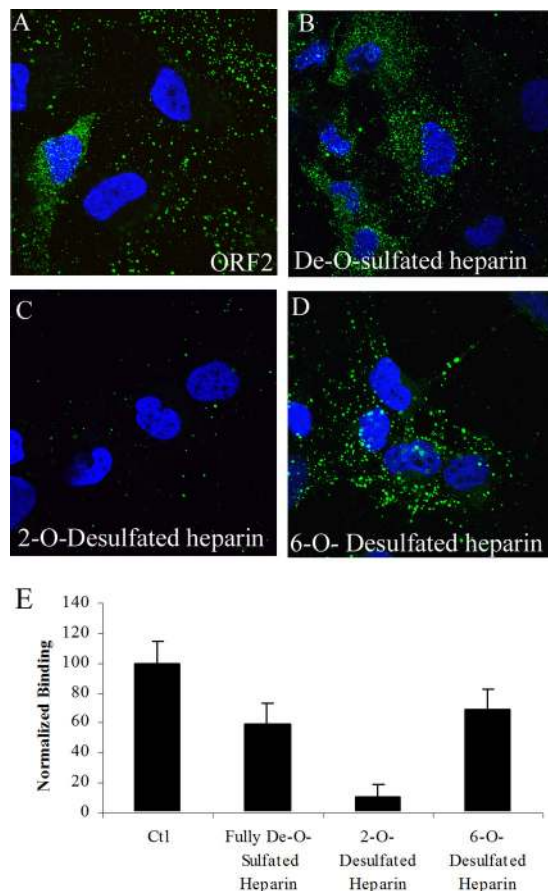


FIG. 7. Effects of differentially sulfated heparins on pORF2 binding. The binding of pORF2 to Huh-7 cells was tested without any addition (A) or in the presence of de-O-sulfated heparin (20 µg/ml) (B), 2-O-desulfated heparin (20 µg/ml) (C), or 6-O-desulfated heparin (20 µg/ml) (D). (E) The binding levels were quantitated as described above and are shown in the bar graph. Ctl, control.

are likely to play a crucial role in promoting HEV infection of target cells, since the removal of cell surface HS by heparinase prevented pORF2 attachment and also blocked HEV infection of Huh-7 cells. The binding appears to be dictated predominantly by HS and not chondroitin sulfates because of reduced inhibition following chondroitinase treatment of cells. Additionally, pORF2 binding could not be suppressed by pretreatment of cells with PIPLC, indicating that the major PG core proteins involved in binding are syndecans and not glypicans. Even though at least four species of PGs were identified by the F69-3G10 Western blot analysis, expressions of only Syndecan-1 and Syndecan-4 were confirmed on Huh-7 cells with type-specific antibodies. Syndecan-1 was the most abundant PG expressed on Huh-7 cells and contributed maximally to pORF2 binding. Syndecan expression is highly regulated and is cell type and developmental-stage specific. A systematic comparison of GAG structures and ligand-binding activities of specific syndecan types has not been reported. In general, HS fine structure appears to reflect the cellular source of the syndecan and not syndecan type-specific differences. Syndecan type-specific function might arise as a consequence of differ-

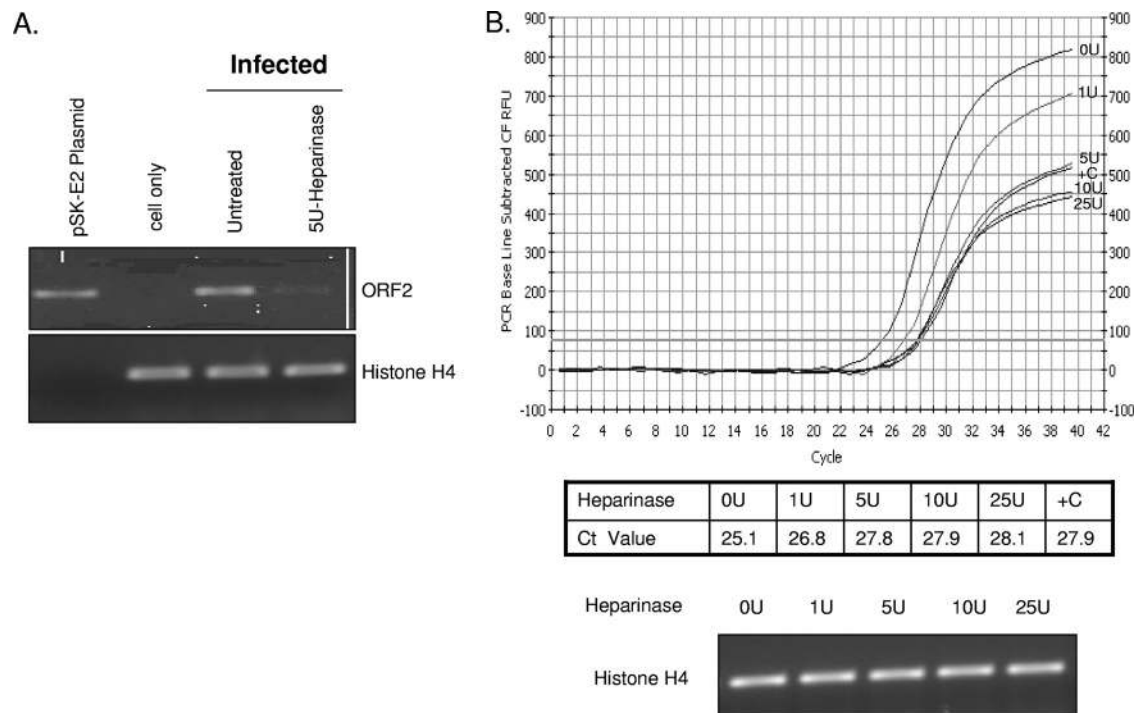


FIG. 8. HSPGs are required for HEV infection of S10-3 cells. Untreated and heparinase I (5 U/ml)-treated S10-3 cells were infected with HEV virions that were produced in replicon-transfected S10-3 cells as described in Materials and Methods. Five days postinfection, RNA was prepared from mock-infected (second lane from the left) or HEV-infected cells (third and fourth lanes), and RT-PCR was performed to estimate the levels of ORF2-expressing transcripts. The pSK-E2 plasmid served as a positive control for PCR. The histone H4 RT-PCR served as a loading control for RNA. (B) S10-3 cells were either left untreated or treated with different amounts of heparinase I and infected with HEV virions. RNA was prepared, real-time RT-PCR was performed using 2  $\mu$ l of first-round PCR mix, and the  $C_T$  value was calculated. The pSK-E2 plasmid served as a positive control for PCR (+C). The histone H4 RT-PCR represents the loading control for RNA.

ences in the orientations and sulfation patterns of the GAG chains displayed on the cell surface (7).

Sulfation levels and patterns on HSPGs are important determinants of interaction of viruses with target cells. Dengue virus and respiratory syncytial virus bind to HS as a function of their degree of sulfation (10, 40). Depending on the tissues and species, HS is highly heterogeneous in terms of both the pattern and level of sulfation, as well as the primary sequences of disaccharides (38, 64). Both heparin and OS-heparin inhibited pORF2 binding to Huh-7 cells by about 80%. HS closely resembles heparin, although the main saccharide unit of HS is slightly different and the degree of sulfation is lower (24). While pORF2 binding could be abrogated by OS-HS, the kidney-derived HS, which has a lower degree of sulfation, did not cause any significant suppression of binding. These results point toward a tropism of HEV for high levels of sulfation found on liver cells; this could be an important determinant in HEV infection of hepatocytes. Compared to HS from other tissues, liver-derived HS has a higher degree of sulfation (64). Increased inhibition of recombinant dengue virus E protein binding to Vero cells by liver-derived HS relative to that from other tissues was observed (10). Highly sulfated liver-specific HS provides binding sites for diverse ligands and receptors (17, 31) and also for various liver-targeting pathogens, like hepatitis C virus (4), dengue virus (10), and *Plasmodium* species (53). Immunochemical studies have also demonstrated the presence of large quantities of HSPGs in the space of Disse in the liver

(61). Thus, it is likely that highly sulfated HSPGs account for the liver tropism of HEV. The relevance of sulfation for pORF2 binding was further substantiated by the observation that inhibition of HSPG sulfation by sodium chlorate reduced pORF2 binding in a dose-dependent manner. Sodium chlorate treatment of cells is known to inhibit HSPG-dependent infection by different viruses (11, 52).

Because HS is one of the most negatively charged molecules, it was important to determine whether pORF2 recognized a specific pattern of sulfate groups on HS or the interaction was a sequence-independent electrostatic one. A growing number of studies suggest that the minimal domains of HS chains required to bind distinct ligands differ from each other (23, 65). The specificity of binding to HSPGs resides mostly in the sulfation pattern of the attached HS chains (14, 59, 66). The chains are generally 50 to 150 disaccharide units in length and can be sulfated at several positions on the disaccharide units (5, 35). Experiments done with chemically modified heparins showed 6-O sulfation to contribute maximally to pORF2 binding to Huh-7 cells. These results provide compelling evidence that the interaction of pORF2 with HSPGs is predominantly mediated by 6-O sulfation. A similar requirement for 6-O sulfation is also seen for the interaction of HIV-1 with syndecans (14). In the case of fibroblast growth factor, 2-O sulfation was shown to be necessary for HIV-1 binding to syndecans, while 6-O sulfation was critical for the formation of a receptor ternary complex (66). The herpesviruses HSV type 1 (HSV-1)

and HSV-2 also differ in their requirements of specific sulfation patterns for binding and entry. While 2,3-O sulfation and 6-O sulfation were critical for the binding of HSV-1 glycoprotein B, this was not the case with HSV-2 glycoproteins (23). Further, even HSV-1 required 3-O sulfation but not 6-O-sulfation for infection (59). However, studies also support the idea that interactions will depend more on the overall organization of HS domains than on their fine structure (31, 49).

We show here that, analogous to many other human viruses, HEV utilizes highly sulfated HS motifs on syndecans to bind to target cells. This interaction was specific, and the removal of HS led to a significant reduction in capsid protein binding as well as infection of cells with HEV. We propose that HEV infects its target cells through a two-step process which involves a low-affinity but high-density interaction with HS followed by a high-affinity interaction with a specific cellular receptor that is yet to be identified. This is the first study to characterize the interactions of the HEV capsid protein with HSPGs on liver cells and show its functional relevance for viral infection.

#### ACKNOWLEDGMENTS

We thank Suzanne Emerson for the HEV infectious replicon, S10-3 cells, and advice on the in vitro infection.

This work was supported by an Innovative Young Biotechnologist Award to M.K. by the Department of Biotechnology (DBT), Government of India. A Senior Research Fellowship to V.C. from the Indian Council of Medical Research is also acknowledged. This work also received valuable support from the Core Imaging Facility at ICGB, New Delhi, India.

#### REFERENCES

1. Ansari, I. H., S. K. Nanda, H. Durgapal, S. Agrawal, S. K. Mohanty, D. Gupta, S. Jameel, and S. K. Panda. 2000. Cloning, sequencing, and expression of the hepatitis E virus (HEV) nonstructural open reading frame 1 (ORF1). *J. Med. Virol.* **60**:275–283.
2. Ashikari-Hada, S., H. Habuchi, Y. Kariya, N. Itoh, A. H. Reddi, and K. Kimata. 2004. Characterization of growth factor-binding structures in heparin/heparan sulfate using an octasaccharide library. *J. Biol. Chem.* **279**:12346–12354.
3. Barth, H., C. Schafer, M. I. Adah, F. Zhang, R. J. Linhardt, H. Toyoda, A. Kinoshita-Toyoda, T. Toida, T. H. Van Kuppevelt, E. Depla, F. Von Weizsacker, H. E. Blum, and T. F. Baumert. 2003. Cellular binding of hepatitis C virus envelope glycoprotein E2 requires cell surface heparan sulfate. *J. Biol. Chem.* **278**:41003–41012.
4. Barth, H., E. K. Schnober, F. Zhang, R. J. Linhardt, E. Depla, B. Bosen, F. L. Cosset, A. H. Patel, H. E. Blum, and T. F. Baumert. 2006. Viral and cellular determinants of the hepatitis C virus envelope-heparan sulfate interaction. *J. Virol.* **80**:10579–10590.
5. Bernfield, M., M. Gotte, P. W. Park, O. Reizes, M. L. Fitzgerald, J. Lincecum, and M. Zako. 1999. Functions of cell surface heparan sulfate proteoglycans. *Annu. Rev. Biochem.* **68**:729–777.
6. Byrnes, A. P., and D. E. Griffin. 1998. Binding of Sindbis virus to cell surface heparan sulfate. *J. Virol.* **72**:7349–7356.
7. Carey, D. J. 1997. Syndecans: multifunctional cell-surface co-receptors. *Biochem. J.* **327**:1–16.
8. Chandra, V., A. Kar-Roy, S. Kumari, S. Mayor, and S. Jameel. 2008. The hepatitis E virus ORF3 protein modulates epidermal growth factor receptor trafficking, STAT3 translocation, and the acute-phase response. *J. Virol.* **82**:7100–7110.
9. Chandra, V., S. Taneja, M. Kalia, and S. Jameel. 2008. Molecular biology and pathogenesis of hepatitis E virus. *J. Biosci.* **33**:451–464.
10. Chen, Y., T. Maguire, R. E. Hileman, J. R. Fromm, J. D. Esko, R. J. Linhardt, and R. M. Marks. 1997. Dengue virus infectivity depends on envelope protein binding to target cell heparan sulfate. *Nat. Med.* **3**:866–871.
11. Chung, C. S., J. C. Hsiao, Y. S. Chang, and W. Chang. 1998. A27L protein mediates vaccinia virus interaction with cell surface heparan sulfate. *J. Virol.* **72**:1577–1585.
12. David, G., B. van der Schueren, P. Marynen, J. J. Cassiman, and H. van den Berghe. 1992. Molecular cloning of amphiglycan, a novel integral membrane heparan sulfate proteoglycan expressed by epithelial and fibroblastic cells. *J. Cell Biol.* **118**:961–969.
13. Dececchi, M. C., A. Tamanini, A. Bonizzato, and G. Cabrini. 2000. Heparan sulfate glycosaminoglycans are involved in adenovirus type 5 and 2-host cell interactions. *Virology* **268**:382–390.
14. de Parseval, A., M. D. Bobardt, A. Chatterji, U. Chatterji, J. H. Elder, G. David, S. Zolla-Pazner, M. Farzan, T. H. Lee, and P. A. Galloway. 2005. A highly conserved arginine in gp120 governs HIV-1 binding to both syndecans and CCR5 via sulfated motifs. *J. Biol. Chem.* **280**:39493–39504.
15. Emerson, S. U., D. Anderson, A. Arankalle, X. J. Meng, M. Purdy, G. G. Schlauder, and S. Tsarev. 2004. *Hepevirus*. Elsevier/Academic Press, London, United Kingdom.
16. Emerson, S. U., H. Nguyen, J. Graff, D. A. Stephany, A. Brockington, and R. H. Purcell. 2004. In vitro replication of hepatitis E virus (HEV) genomes and of an HEV replicon expressing green fluorescent protein. *J. Virol.* **78**:4838–4846.
17. Esko, J. D., and U. Lindahl. 2001. Molecular diversity of heparan sulfate. *J. Clin. Investig.* **108**:169–173.
18. Fry, E. E., S. M. Lea, T. Jackson, J. W. Newman, F. M. Ellard, W. E. Blakemore, R. Abu-Ghazaleh, A. Samuel, A. M. King, and D. I. Stuart. 1999. The structure and function of a foot-and-mouth disease virus-oligosaccharide receptor complex. *EMBO J.* **18**:543–554.
19. Graff, J., U. Torian, H. Nguyen, and S. U. Emerson. 2006. A bicistronic subgenomic mRNA encodes both the ORF2 and ORF3 proteins of hepatitis E virus. *J. Virol.* **80**:5919–5926.
20. Graff, J., Y. H. Zhou, U. Torian, H. Nguyen, M. St. Claire, C. Yu, R. H. Purcell, and S. U. Emerson. 2008. Mutations within potential glycosylation sites in the capsid protein of hepatitis E virus prevent the formation of infectious virus particles. *J. Virol.* **82**:1185–1194.
21. Guu, T. S., Z. Liu, Q. Ye, D. A. Mata, K. Li, C. Yin, J. Zhang, and Y. J. Tao. 2009. Structure of the hepatitis E virus-like particle suggests mechanisms for virus assembly and receptor binding. *Proc. Natl. Acad. Sci. USA* **106**:12992–12997.
22. Haqshenas, G., and X. J. Meng. 2001. Determination of the nucleotide sequences at the extreme 5' and 3' ends of swine hepatitis E virus genome. *Arch. Virol.* **146**:2461–2467.
23. Herold, B. C., S. I. Gerber, B. J. Belval, A. M. Siston, and N. Shulman. 1996. Differences in the susceptibility of herpes simplex virus types 1 and 2 to modified heparin compounds suggest serotype differences in viral entry. *J. Virol.* **70**:3461–3469.
24. Hileman, R. E., J. R. Fromm, J. M. Weiler, and R. J. Linhardt. 1998. Glycosaminoglycan-protein interactions: definition of consensus sites in glycosaminoglycan binding proteins. *Bioessays* **20**:156–167.
25. Hilgard, P., and R. Stockert. 2000. Heparan sulfate proteoglycans initiate dengue virus infection of hepatocytes. *Hepatology* **32**:1069–1077.
26. Huang, Y. W., T. Oppriessnig, P. G. Halbur, and X. J. Meng. 2007. Initiation at the third in-frame AUG codon of open reading frame 3 of the hepatitis E virus is essential for viral infectivity in vivo. *J. Virol.* **81**:3018–3026.
27. Jameel, S., M. Zafrullah, M. H. Ozden, and S. K. Panda. 1996. Expression in animal cells and characterization of the hepatitis E virus structural proteins. *J. Virol.* **70**:207–216.
28. Kim, C. W., O. A. Goldberger, R. L. Gallo, and M. Bernfield. 1994. Members of the syndecan family of heparan sulfate proteoglycans are expressed in distinct cell-, tissue-, and development-specific patterns. *Mol. Biol. Cell* **5**:797–805.
29. Korkaya, H., S. Jameel, D. Gupta, S. Tyagi, R. Kumar, M. Zafrullah, M. Mazumdar, S. K. Lal, L. Xiaofang, D. Sehgal, S. R. Das, and D. Sahal. 2001. The ORF3 protein of hepatitis E virus binds to Src homology 3 domains and activates MAPK. *J. Biol. Chem.* **276**:42389–42400.
30. Krawczynski, K., R. Aggarwal, and S. Kamili. 2000. Hepatitis E. *Infect. Dis. Clin. N. Am.* **14**:669–687.
31. Kreuger, J., D. Spillmann, J. P. Li, and U. Lindahl. 2006. Interactions between heparan sulfate and proteins: the concept of specificity. *J. Cell Biol.* **174**:323–327.
32. Krusat, T., and H. J. Streckert. 1997. Heparin-dependent attachment of respiratory syncytial virus (RSV) to host cells. *Arch. Virol.* **142**:1247–1254.
33. Li, S., X. Tang, J. Seetharaman, C. Yang, Y. Gu, J. Zhang, H. Du, J. W. Shih, C. L. Hew, J. Sivaraman, and N. Xia. 2009. Dimerization of hepatitis E virus capsid protein E2s domain is essential for virus-host interaction. *PLoS Pathog.* **5**:e1000537.
34. Li, T. C., Y. Yamakawa, K. Suzuki, M. Tatsumi, M. A. Razak, T. Uchida, N. Takeda, and T. Miyamura. 1997. Expression and self-assembly of empty virus-like particles of hepatitis E virus. *J. Virol.* **71**:7207–7213.
35. Lindahl, U., M. Kusche-Gullberg, and L. Kjellen. 1998. Regulated diversity of heparan sulfate. *J. Biol. Chem.* **273**:24979–24982.
36. Lohse, D. L., and R. J. Linhardt. 1992. Purification and characterization of heparin lyases from *Flavobacterium heparinum*. *J. Biol. Chem.* **267**:24347–24355.
37. Lyon, M., and J. T. Gallagher. 1998. Bio-specific sequences and domains in heparan sulphate and the regulation of cell growth and adhesion. *Matrix Biol.* **17**:485–493.
38. Maccarana, M., Y. Sakura, A. Tawada, K. Yoshida, and U. Lindahl. 1996. Domain structure of heparan sulfates from bovine organs. *J. Biol. Chem.* **271**:17804–17810.

39. Mandl, C. W., H. Kroschewski, S. L. Allison, R. Kofler, H. Holzmann, T. Meixner, and F. X. Heinz. 2001. Adaptation of tick-borne encephalitis virus to BHK-21 cells results in the formation of multiple heparan sulfate binding sites in the envelope protein and attenuation in vivo. *J. Virol.* **75**:5627–5637.
40. Martínez, I., and J. A. Melero. 2000. Binding of human respiratory syncytial virus to cells: implication of sulfated cell surface proteoglycans. *J. Gen. Virol.* **81**:2715–2722.
41. McClain, D. S., and A. O. Fuller. 1994. Cell-specific kinetics and efficiency of herpes simplex virus type 1 entry are determined by two distinct phases of attachment. *Virology* **198**:690–702.
42. Meng, X. J. 2009. Hepatitis E virus: animal reservoirs and zoonotic risk. *Vet. Microbiol.* [Epub ahead of print.] doi:10.1016/j.vetmic.2009.03.017.
43. Meng, X. J., R. H. Purcell, P. G. Halbur, J. R. Lehman, D. M. Webb, T. S. Tsareva, J. S. Haynes, B. J. Thacker, and S. U. Emerson. 1997. A novel virus in swine is closely related to the human hepatitis E virus. *Proc. Natl. Acad. Sci. USA* **94**:9860–9865.
44. Moin, S. M., M. Panteva, and S. Jameel. 2007. The hepatitis E virus Orf3 protein protects cells from mitochondrial depolarization and death. *J. Biol. Chem.* **282**:21124–21133.
45. Mondor, I., S. Ugolini, and Q. J. Sattentau. 1998. Human immunodeficiency virus type 1 attachment to HeLa CD4 cells is CD4 independent and gp120 dependent and requires cell surface heparans. *J. Virol.* **72**:3623–3634.
46. Nader, H. B., C. P. Dietrich, V. Buonassisi, and P. Colburn. 1987. Heparin sequences in the heparan sulfate chains of an endothelial cell proteoglycan. *Proc. Natl. Acad. Sci. USA* **84**:3565–3569.
47. Panda, S. K., I. H. Ansari, H. Durgapal, S. Agrawal, and S. Jameel. 2000. The in vitro-synthesized RNA from a cDNA clone of hepatitis E virus is infectious. *J. Virol.* **74**:2430–2437.
48. Piñon, J. D., P. J. Klasse, S. R. Jassal, S. Welson, J. Weber, D. W. Brighty, and Q. J. Sattentau. 2003. Human T-cell leukemia virus type 1 envelope glycoprotein gp46 interacts with cell surface heparan sulfate proteoglycans. *J. Virol.* **77**:9922–9930.
49. Powell, A. K., E. A. Yates, D. G. Fernig, and J. E. Turnbull. 2004. Interactions of heparin/heparan sulfate with proteins: appraisal of structural factors and experimental approaches. *Glycobiology* **14**:17R–30R.
50. Pudupakam, R. S., Y. W. Huang, T. Opriessnig, P. G. Halbur, F. W. Pierson, and X. J. Meng. 2009. Deletions of the hypervariable region (HVR) in open reading frame 1 of hepatitis E virus do not abolish virus infectivity: evidence for attenuation of HVR deletion mutants in vivo. *J. Virol.* **83**:384–395.
51. Putnak, J. R., N. Kanesa-Thanas, and B. L. Innis. 1997. A putative cellular receptor for dengue viruses. *Nat. Med.* **3**:828–829.
52. Qiu, J., A. Handa, M. Kirby, and K. E. Brown. 2000. The interaction of heparin sulfate and adeno-associated virus 2. *Virology* **269**:137–147.
53. Rathore, D., T. F. McCutchan, D. N. Garboczi, T. Toida, M. J. Hernaiz, L. A. LeBrun, S. C. Lang, and R. J. Linhardt. 2001. Direct measurement of the interactions of glycosaminoglycans and a heparin decasaccharide with the malaria circumsporozoite protein. *Biochemistry* **40**:11518–11524.
54. Riddell, M. A., F. Li, and D. A. Anderson. 2000. Identification of immunodominant and conformational epitopes in the capsid protein of hepatitis E virus by using monoclonal antibodies. *J. Virol.* **74**:8011–8017.
55. Robinson, R. A., W. H. Burgess, S. U. Emerson, R. S. Leibowitz, S. A. Sosnovtseva, S. Tsarev, and R. H. Purcell. 1998. Structural characterization of recombinant hepatitis E virus ORF2 proteins in baculovirus-infected insect cells. *Protein Expr. Purif.* **12**:75–84.
56. Ropp, S. L., A. W. Tam, B. Beames, M. Purdy, and T. K. Frey. 2000. Expression of the hepatitis E virus ORF1. *Arch. Virol.* **145**:1321–1337.
57. Sehgal, D., P. S. Malik, and S. Jameel. 2003. Purification and diagnostic utility of a recombinant hepatitis E virus capsid protein expressed in insect larvae. *Protein Expr. Purif.* **27**:27–34.
58. Shieh, M. T., D. WuDunn, R. I. Montgomery, J. D. Esko, and P. G. Spear. 1992. Cell surface receptors for herpes simplex virus are heparan sulfate proteoglycans. *J. Cell Biol.* **116**:1273–1281.
59. Shukla, D., J. Liu, P. Blaiklock, N. W. Shworak, X. Bai, J. D. Esko, G. H. Cohen, R. J. Eisenberg, R. D. Rosenberg, and P. G. Spear. 1999. A novel role for 3-O-sulfated heparan sulfate in herpes simplex virus 1 entry. *Cell* **99**:13–22.
60. Shukla, D., and P. G. Spear. 2001. Herpesviruses and heparan sulfate: an intimate relationship in aid of viral entry. *J. Clin. Investig.* **108**:503–510.
61. Stow, J. L., L. Kjellen, E. Unger, M. Hook, and M. G. Farquhar. 1985. Heparan sulfate proteoglycans are concentrated on the sinusoidal plasmalemmal domain and in intracellular organelles of hepatocytes. *J. Cell Biol.* **100**:975–980.
62. Tam, A. W., M. M. Smith, M. E. Guerra, C. C. Huang, D. W. Bradley, K. E. Fry, and G. R. Reyes. 1991. Hepatitis E virus (HEV): molecular cloning and sequencing of the full-length viral genome. *Virology* **185**:120–131.
63. Tamura, M., K. Natori, M. Kobayashi, T. Miyamura, and N. Takeda. 2004. Genogroup II noroviruses efficiently bind to heparan sulfate proteoglycan associated with the cellular membrane. *J. Virol.* **78**:3817–3826.
64. Toida, T., H. Yoshida, H. Toyoda, I. Koshiishi, T. Imanari, R. E. Hileman, J. R. Fromm, and R. J. Linhardt. 1997. Structural differences and the presence of unsubstituted amino groups in heparan sulphates from different tissues and species. *Biochem. J.* **322**:499–506.
65. Trybala, E., J. A. Liljeqvist, B. Svennerholm, and T. Bergstrom. 2000. Herpes simplex virus types 1 and 2 differ in their interaction with heparan sulfate. *J. Virol.* **74**:9106–9114.
66. Wang, S., X. Ai, S. D. Freeman, M. E. Pownall, Q. Lu, D. S. Kessler, and C. P. Emerson, Jr. 2004. QSulf1, a heparan sulfate 6-O-endosulfatase, inhibits fibroblast growth factor signaling in mesoderm induction and angiogenesis. *Proc. Natl. Acad. Sci. USA* **101**:4833–4838.
67. WuDunn, D., and P. G. Spear. 1989. Initial interaction of herpes simplex virus with cells is binding to heparan sulfate. *J. Virol.* **63**:52–58.
68. Yamagata, T., H. Saito, O. Habuchi, and S. Suzuki. 1968. Purification and properties of bacterial chondroitinases and chondrosulfatases. *J. Biol. Chem.* **243**:1523–1535.
69. Yamashita, T., Y. Mori, N. Miyazaki, R. H. Cheng, M. Yoshimura, H. Unno, R. Shima, K. Moriishi, T. Tsukihara, T. C. Li, N. Takeda, T. Miyamura, and Y. Matsuura. 2009. Biological and immunological characteristics of hepatitis E virus-like particles based on the crystal structure. *Proc. Natl. Acad. Sci. USA* **106**:12986–12991.
70. Zafrullah, M., M. H. Ozdener, R. Kumar, S. K. Panda, and S. Jameel. 1999. Mutational analysis of glycosylation, membrane translocation, and cell surface expression of the hepatitis E virus ORF2 protein. *J. Virol.* **73**:4074–4082.
71. Zhou, Y. H., R. H. Purcell, and S. U. Emerson. 2004. An ELISA for putative neutralizing antibodies to hepatitis E virus detects antibodies to genotypes 1, 2, 3, and 4. *Vaccine* **22**:2578–2585.